Electrochemical methods for determining diffusion coefficient of hydrogen in steels

G. Fumagalli[1], F. Bolzoni*[1], E. Fallahmohammadi[2], G. Re[1] and L. Lazzari[1]

Introduction

Owing to its small size, atomic hydrogen can enter metallic materials when produced by corrosion processes, in the presence of poisons for hydrogen recombination such as H_2S, and during galvanic surface treatments or cathodic protection, as well as from high pressure hydrogen gas. By interacting with the microstructure, hydrogen can cause embrittlement of susceptible materials, such as bcc (ferritic) steels, which are the most widely used in industry.[1]

The diffusion of a chemical species in a medium is described by Fick's laws. In particular, the standardised test for measuring diffusion, ISO 17081, applies a Fourier numerical solution of Fick's second law.[2–5] The mathematical models of diffusion developed by some authors[6–14] are more complex, considering trapping phenomena as a set of reversible or irreversible reactions, each characterised by its own kinetics and equilibrium conditions. Moreover, when the mobility of hydrogen is relatively high (e.g. in iron or ferritic steels), the permeation rate may be affected also by surface processes involving hydrogen entry.

Therefore, the experimental outcome of a diffusion test in accordance with ISO 17081 cannot be processed using Fick's law alone, unless one operates in such a way as to minimise the effects of hydrogen interaction with traps as proposed by Turnbull *et al.*[3,15] or Zakroczymski.[16,17]

[1]Dipartimento di Chimica, Materiali e Ingegneria Chimica G. Natta, Politecnico di Milano, Via Mancinelli 7, Milan 20131, Italy
[2]Prysmian S.p.A. Viale Sarca 222, Milan 20126, Italy
*Corresponding author, email fabio.bolzoni@polimi.it

Received 18 December 2014; accepted 17 February 2015

With regard to the physical model, it should be stressed that the transport of absorbed hydrogen atoms (H_{abs}) depends not only on time, the geometry of the membrane and the crystal lattice of the material but, above all, on the actual metallurgical microstructure, i.e. on the presence and distribution of all phases and lattice defects with which the permeating hydrogen can interact. For example, in C–Mn steels with ferritic (bcc) or martensitic (bct) structure, we can have phases such as carbides and inclusions of various types, point lattice defects (vacancies and interstitial and substitutional atoms), line defects (dislocations), surface defects (grain boundaries), etc. We call a 'trap' anything that interacts with the permeating hydrogen, stressing the fact that interactions may be of different types and intensity, so we can distinguish traps according to the following indications.

First are the cavities of the ideal lattice without defects (interstitial sites in the metal lattice $= T_{IML}$), with which hydrogen forms a bond characterised, at ordinary temperatures, by low activation energies for capture and release and by low binding energy. This hydrogen diffusion process is 'fast' and it is the one that acts within grains with little deformation, i.e. with low dislocation density.

Second are the other phases or lattice defects with which hydrogen forms bonds characterised by very high binding energy and high activation energy for the hydrogen release: these traps are defined as 'irreversible' T_{irr} because, at ordinary temperatures, part of the hydrogen cannot be released. As long as these traps are active, the flux of hydrogen is slowed, depending on their type, number and distribution, and its value also depends on the different capture rates $v_{irr,cap}$ and time. Once the T_{irr} are saturated ($v_{irr,cap} = 0$), the flux of hydrogen is no longer influenced by

their presence. In addition, in some cases, non-saturable traps may be formed, e.g. blisters.

Third are lattice defects such as vacancies, dislocations or grain boundaries (reversible traps T_{rev}), with which the hydrogen forms bonds that are characterised by binding energy and activation energies for capture/release that are generally higher than those for T_{IML}: the flux of part of the hydrogen is slowed in its migration process depending on their type, number and distribution and on the different capture/release rates ($v_{rev,cap}$ and $v_{rev,rel}$). Until the reversible traps reach a steady state ($v_{rev,cap} = v_{rev,rel}$ specific to each type of trap), the flux of hydrogen cannot be considered steady.

Fourth are the interstitial sites plus reversible traps-with higher capture/release rates ($T_L = T_{IML} + T_{rev1} + T_{rev2} + ...$), which must necessarily be crossed to allow steady state migration of hydrogen: these kinds of traps reach their equilibrium conditions very rapidly and the diffusion process is the 'fastest' that is possible for a specific material. The flux of hydrogen will be constant under the boundary conditions of diffusion tests when all the T_{irr} are saturated ($v_{irr,cap} = 0$) and when all the T_{rev} reach their steady state. Under steady state flux conditions, the material will be characterised by a diffusion coefficient D_L.

Figure 1 shows the above model in schematic form, without considering non-saturable traps. According to this model, the measured hydrogen flux and the resulting diffusion coefficient depend on the experimental conditions. In fact, the stationary conditions for the different traps depend also on the activity of absorbed hydrogen, which is linked to:

(i) the value of the cathodic current i_c
(ii) the presence of inhibitors of the reaction for the formation of H_2 (e.g. sulphides)
(iii) the fluid dynamical conditions on the electrode surface
(iv) the physicochemical conditions on the electrode surface.

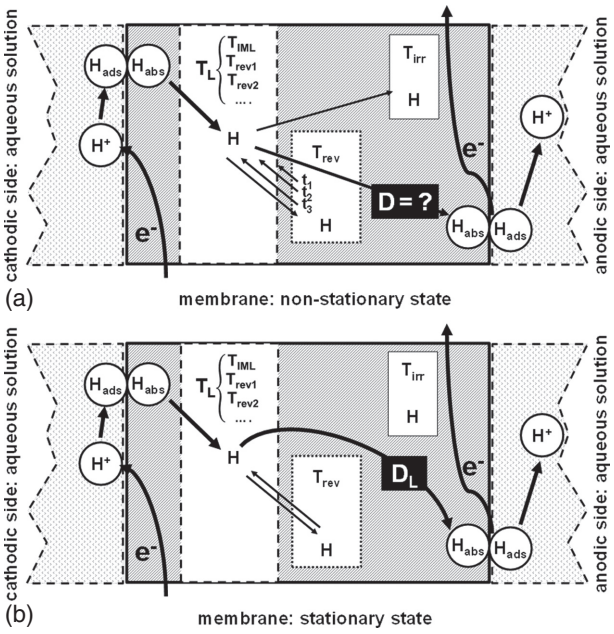

1 Schematic representation of model for transport of hydrogen in the metallic membrane in *a* non-stationary and *b* stationary states of trapping processes

The hydrogen diffusion is thus characterised by a lattice diffusion coefficient D_L that is not measurable on a real material before cathodic surface (hydrogen entry) and all trapping phenomena have reached steady state.[15–17] The value of the 'apparent' D that can be estimated experimentally in non-steady state conditions (e.g. in the first tens of hours of polarisation) can:

(i) be a function of the time during the permeation transient at which the estimate is made;
(ii) be poorly reproducible because of the non-stationary conditions of the cathodic surface and complex interactions with the traps, which vary with time and space;
(iii) be lower or much lower than the lattice diffusion coefficient.

On the other hand, if, after a steady state has been reached for all processes involved in hydrogen transport, a small flux variation is performed, then a new steady state can be attained in a short time, without altering the trapping equilibrium and with Fick's second law being obeyed. In this way, it is possible to measure the correct value of D_L.

In the context of basic research on this topic, with the consequences of hydrogen diffusion on mechanical properties having already been examined,[18–20] electrochemical methods have been applied to determine the diffusion coefficient of hydrogen inside two steels used for sour hydrocarbon transport.[21,22] The ISO 17081 standard[5] and the method proposed by Zakroczymski[16,17] have been compared. Three metallurgical structures of C–Mn microalloyed steel of API 5L X65 grade and low alloy 2·25Cr–1Mo steel of ASTM A182 F22 grade, properly annealed, quenched and tempered (sour service grade) and water quenched (WQ) have been tested.[23] In addition, as received and cold worked low alloy steel of X65 grade, with different degrees of plastic deformation obtained by rolling, have also been tested.[24]

Experimental

The electrochemical method used is the Devanathan–Stachurski double cell method,[2] referenced in ISO 17081,[5] with appropriate procedural modifications as suggested by Zakroczymski.[16,17] The details of the apparatus, the selected test parameters, the materials and the surface treatments are discussed in a previous paper;[23] here, we merely stress the following points.

First, the materials used for these tests comply with the API 5L X65 and ASTM A182 F22 specifications,[25,26] and they were tested in three different metallurgical structures obtained by heat treatment by the manufacturer [quenching and tempering (Q&T)] or in the laboratory [annealing (A) and water quenching (WQ)]. Table 1 shows the chemical compositions, and Table 2 shows the thermal treatment and hardness. Figure 2 shows the metallurgical microstructures for the two materials: further details of the microstructures are given by Fallahmohammadi *et al.*[23] Each sample of each material consisted of three specimens (1–3). In addition, samples of X65 steel Q&T at different degrees of plastic deformation obtained by tensile testing or cold rolling (6, 22 and 43%) were investigated.[24]

Second, the cathodic solution had a chemical composition of 0·4 mol L^{-1} CH_3COOH + 0·2 mol L^{-1}

Table 1 Chemical compositions/wt-%

Steel	C	Mn	S	Mo	Cr	Ni	Nb	V	Ti
X65	0·11	1·18	0·007	0·15	0·17	0·42	0·023	<0·06	<0·01
F22	0·14	0·43	0·001	1·04	2·25	0·08	0·02	<0·01	<0·01

Table 2 Heat treatment and hardness

Material	Sample	Heat treatment	Microhardness/HV
X65	A	930°C/30 min furnace cooled	150±18
	Q&T	As received	206±8
	WQ	930°C/30 min water quenched	433±33
F22	A	930°C/30 min furnace cooled	170±11
	Q&T	As received	211±4
	WQ	930°C/30 min water quenched	478±15

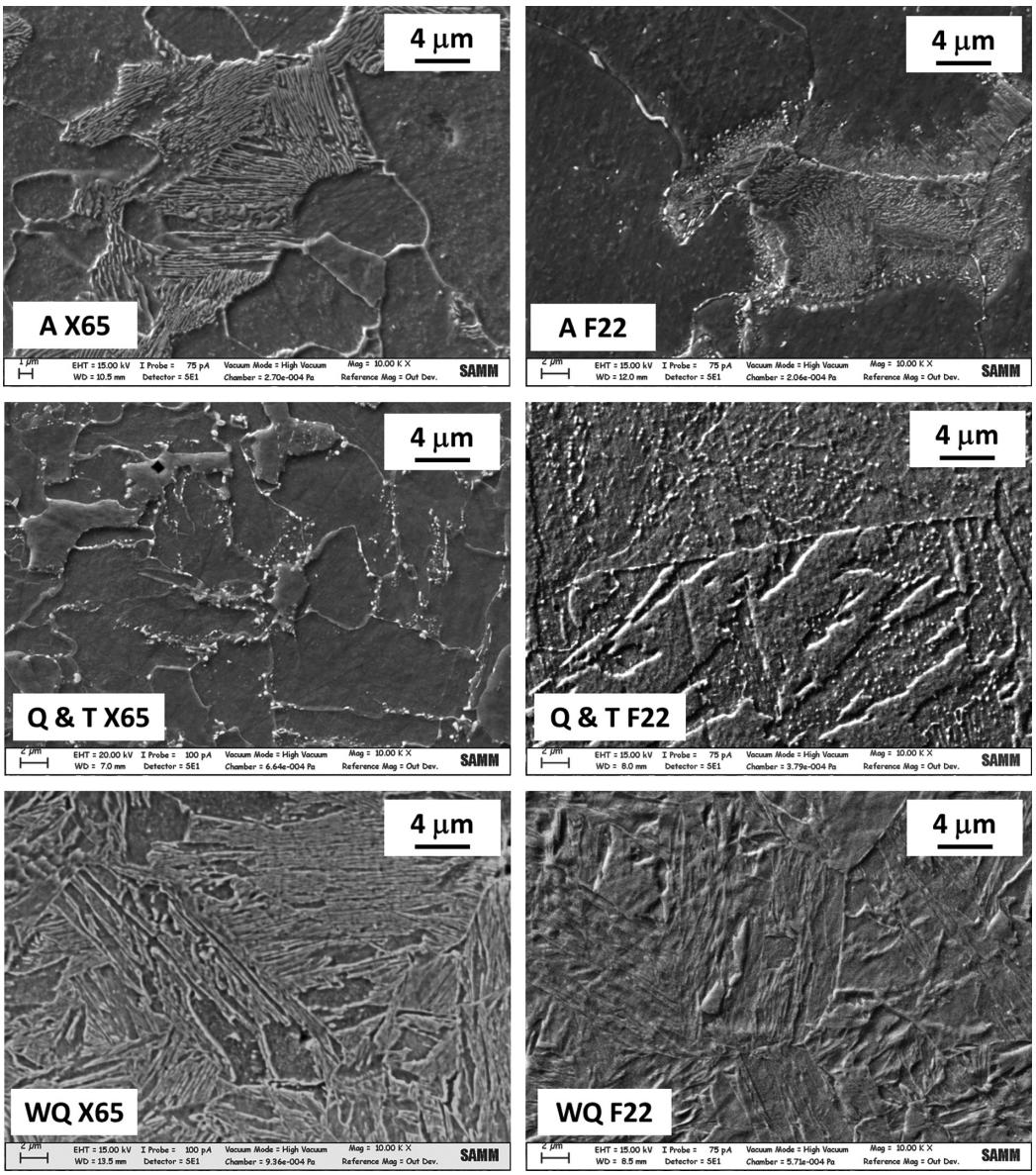

2 Images (SEM) of steel microstructures: annealed (ferrite grains and islands of pearlite in A X65; same with chromium carbide precipitate in grain boundaries in AF22), quenched and tempered (ferrite with finely dispersed carbides in Q&T X65; same with mixed tempered martensite in Q&T F22), water quenched (martensite in WQ X65 and WQ F22)

CH_3COONa (buffered at pH ~4). The solution flowed on the electrode (~1 m s^{-1}) and was drawn from a 5 L tank, where it was deoxygenated with N_2; galvanostatic polarisation was carried out at $i_c = -0{\cdot}5$ mA cm^{-2}. These choices were made in order to have a pH similar to that of a 'sour' environment and to maintain stable pH conditions on the electrode during the test; the cathodic current density was selected in order to guarantee complete protection of the steel without provoking visible bubbling of hydrogen (H_2) on the steel surface.

Third, the anodic solution had a chemical composition of 0·2 mol L^{-1} NaOH (pH >13) and was stagnant. Potentiostatic polarisation was carried out at E_a(Ag/AgCl/3 mol L^{-1} KCl/) = +0·10 V. Membranes were coated with palladium with the aim of guaranteeing almost complete oxidation of the permeating hydrogen.[5,27–29]

Fourth, the entire system was thermostated at 20 ± 2°C, and the solutions were replaced at the end of each test.

Fifth, the results were evaluated and compared using different experimental methods: in particular, with the first and second charge method (char1 and char2) according to ISO 17081,[5] with the partial charge and discharge method (p.char1/2 and p.dis1/2) according to Zakroczymski[16,17] and with the full discharge method (dis1 and dis2).[16,17,30]

The test results are represented here as i_a/i_{max} versus time/L^2 graphs, which means that the current density is divided by the maximum current density reached during its respective permeation history (a dimensionless parameter), and time is divided by the square of the sample thickness (not a dimensionless parameter). In this way, any dependence of experimental data on maximum current peak or sample thickness is eliminated. Moreover, using the time/L^2 parameter allows easy comparison of diffusion coefficients measured in different tests, the distance between the experimental curves along the x-axis being equal to the ratio between the diffusion coefficients.

A logarithmic scale is used on the x-axis both to provide a better visualisation of the rapid changes that take place over relatively short times, compressing the slower ones that take place over relatively long times and because of the symmetry assumed by the Fick's law theoretical curves with this representation.

Figure 3*a* shows a theoretical curve according to Fick's law with an arbitrary value of D for a generic positive anodic current transient (char): for higher values of D, the curve shifts to the left, whereas for lower ones, it shifts to the right. Figure 3*b* shows the theoretical curve for the discharge transient, represented by plotting on the y-axis the experimental values as a function of i_a/i_{max} (thin line = dis′). If the results are plotted as a function of $1-i_a/i_{max}$ (thick line = dis), a comparison between the charge and discharge phases (char or dis) can easily be made by simple superposition of the curves in the different phases.

The same representation has been used for the partial charge/discharge tests, putting for the latter on the y-axis the quantity $\Delta i_a/\Delta i_{max}$ and on the x-axis the normalised time given by time/L^2. The Δi values are calculated starting from the steady state current reached in the previous phase of the test, and the normalised time is measured from the change in the imposed cathodic current i_c.

Results and discussion

Test procedure

The test procedure adopted for each specimen can be described in terms of the following steps.

First, after anode stabilisation, the cathodic compartment is filled with a flowing acetate solution, the cathode is polarised at a current density $i_c = -0{\cdot}5$ mA cm^{-2} and the test is started at this instant ($t = 0$ s). The anodic current density i_a remains relatively constant around the value of the passivation current i_a* (less than tenths of μA cm^{-2}), until the arrival of the first hydrogen atoms on the anode: the contribution of hydrogen oxidation to the anodic current density is thus represented by $i_{aH} = i_a - i_a$*.

This initial period can last from a minimum of ~10 min to a few hours, depending on the type of sample (A, Q&T or WQ) and on the thickness of the specimen.

Second, after the period of step 1, i_a tends to rise rapidly (Fig. 4*a*) with a more or less steep slope tending to a nearly constant value (Fig. 4*b*). After a few hours, the anodic current i_a becomes more than one order of magnitude higher than the passivation current i_a*, so the latter can be completely neglected for the calculation of the hydrogen flux (i.e. $i_{a,H} = i_a$). Above a certain value of i_a, the current increase tends to slow down; stationary conditions are reached after ~100 h.

In some cases, the anodic current, after reaching a peak, decreases and then rises again, as shown, for example, in char2 of Fig. 4*b*. These 'maximum trends' are plausibly related to slow trapping phenomena: some of the reversible traps release hydrogen that has been previously captured, thus causing a temporary increase

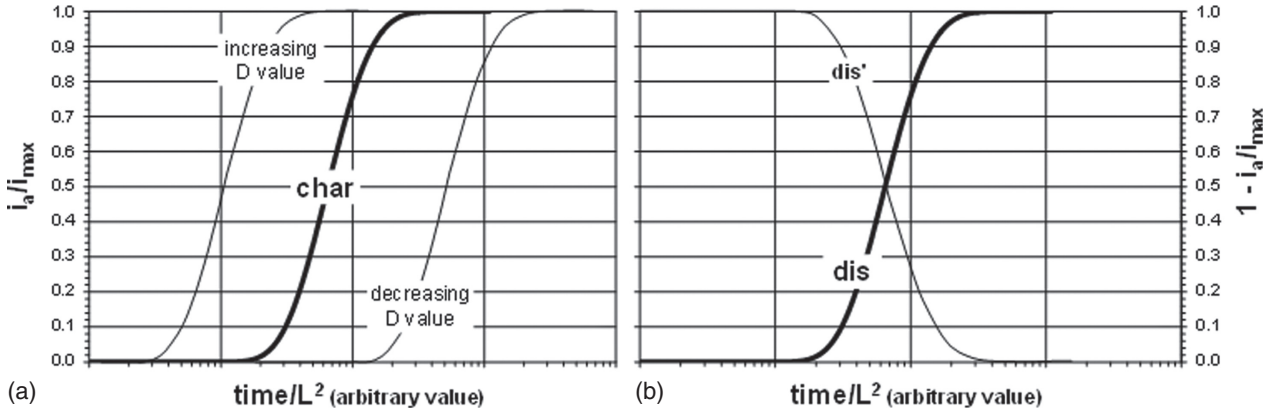

a for char1, i_a/i_{max} versus time/L_2 (arbitrary values) and *b* for dis1, $1-i_a/i_{max}$ versus time/L_2 (arbitrary values)

3 Theoretical curves in accordance with Fick's second law and with boundary conditions for its solution

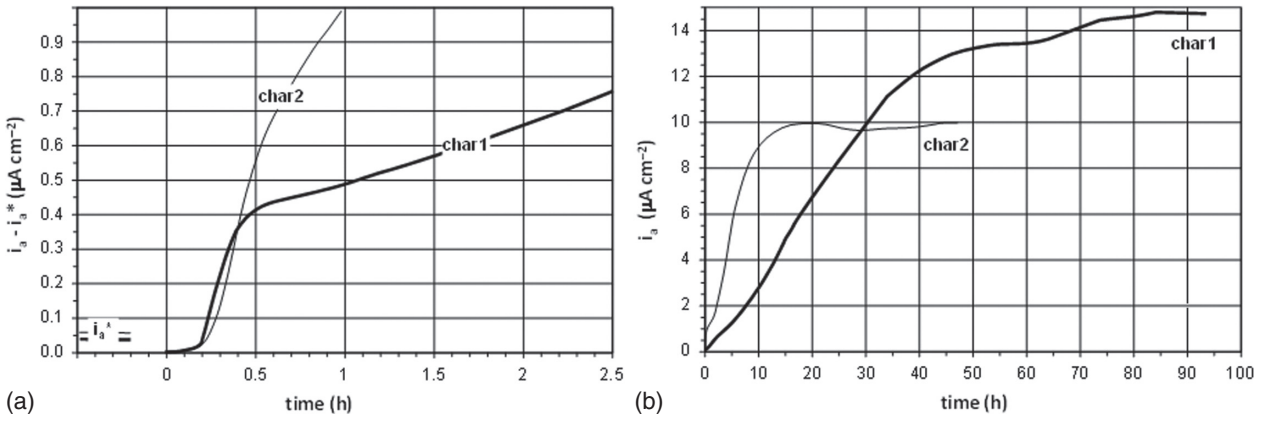

a -0.5–2.5 h; *b* 0–100 h

4 Diagram of anodic current density versus time for specimen A3 (X65 annealed; thickness, 1·03 mm) after cathodic polarisation (char1: first charge test; char2: repeated charge test)

in current up to a maximum value. Then, when other traps enter into play (at a slower capture rate than those previously active), i_a decreases with a more or less pronounced deceleration to a minimum value. This type of irregular permeation curve has already been reported in the literature for different materials and environments.[31–34]

When changes in i_a over time are small, the system can be deemed to be in a steady state; this generally occurs after approximately 80–100 h for char1 and after $\sim$50 h for char2: in char1, both reversible and irreversible traps are active, whereas in char2, only reversible traps are active because the irreversible ones have already saturated during char1, so the steady state can be reached in a shorter time.[3,15]

Third, once the diffusion process has approached steady state conditions, i.e. when i_a has tended to a constant value, the hydrogen entry conditions should also be constant. It is therefore possible to take some measurements while maintaining the boundary conditions of Fick's second law. For example, we can vary the cathodic current density i_c and then measure a new transient of i_a related to these specific conditions. In particular, it has been observed that the duration and intensity of this change in the system must be sufficiently smaller than those necessary to induce variations also in the steady state. This is possible because the capture processes of the T_{rev} are slower than the diffusion processes of hydrogen. Experimentally, after $\sim$100 h of cathodic polarisation and going from a value of $i_c = -0{\cdot}5$ to -1 mA cm^{-2}, and vice versa going from $i_c = -1$ to $-0{\cdot}5$ mA cm^{-2}, it is possible to obtain a measurement of i_a (Fig. 5*a*) that will allow us to process data obtained at steady state. This double transition has been called the partial charge and partial discharge phase (p.char1, p.dis1). In $\sim$30 s, it is possible to detect the start of the anodic current variation induced by the changes occurred at the cathode on the type A sample (Fig. 5*a*). After p.char and p.dis, the measured anodic current is only slightly lower (about -5%) than the steady state current (Fig. 5*a*). The curves of the anodic current transients obtained with the partial charge/discharge method are fairly symmetrical with respect to each other, and, as will be more readily apparent in Fig. 6, they follow Fick's second law perfectly, allowing us to obtain a good estimate of the diffusion coefficient D_L.

Fourth, the last phase of the measurement of i_a, namely that pertaining to the variation in cathodic current density i_c from $-0{\cdot}5$ to 0 mA cm^{-2}, is called 'discharge' (dis1 or dis2 in the repeated test) because almost all absorbed hydrogen, apart from what has become irreversibly trapped, escapes from the metallic membrane from both surfaces (Fig. 5*b*). In the case of flux controlled by Fick's second law, according to the model of Nanis and Namboodhiri,[30] the quantity of hydrogen exiting from the anodic surface is approximately one third of the total, and obviously the other two thirds escapes from the cathodic surface, where measurements cannot be taken in our experimental set-up.

After the current has been switched off, the measured anodic current remains constant for a relatively short period (tens of seconds in the case of the A3 specimen). Then, i_a decreases, following, at least from 100 to 90% of i_{max} (a few minutes for A3 in Fig. 5*b*), the trend predicted by Fick's second law with a suitable value of D_L (as we will see more clearly in Fig. 6). In this regard, the same considerations regarding the D_L obtained with the p.char/p.dis method also apply: in fact, the values of D_L estimated with the two methods are rather close. During a discharge transient starting from a steady state of flux, the first measured data meet the condition of Fick's law diffusion before the occurrence of the phenomenon of progressive release of hydrogen from the reversible traps.[16,17]

In a second period of discharge, which is far longer than the previous one, a current greater than that predicted by Fick's second law is measured, owing to the release of hydrogen by the reversible traps. The discharge phase ends when the anodic current reaches values of the order of magnitude of the passivity current. In particular, we can observe that the order of magnitude of the times is $\sim$100 h, providing evidence that the rates of release of hydrogen from these traps are slow.

With respect to the test procedure in the discharge phases, it must be stressed that, at the beginning of the discharge, the flowrate of the cathodic solution has to be maintained to avoid disturbing the measurement of hydrogen flux (the current peaks around tenths of an hour in Fig. 5*b*). Only when i_a assumes values $<$70–80%

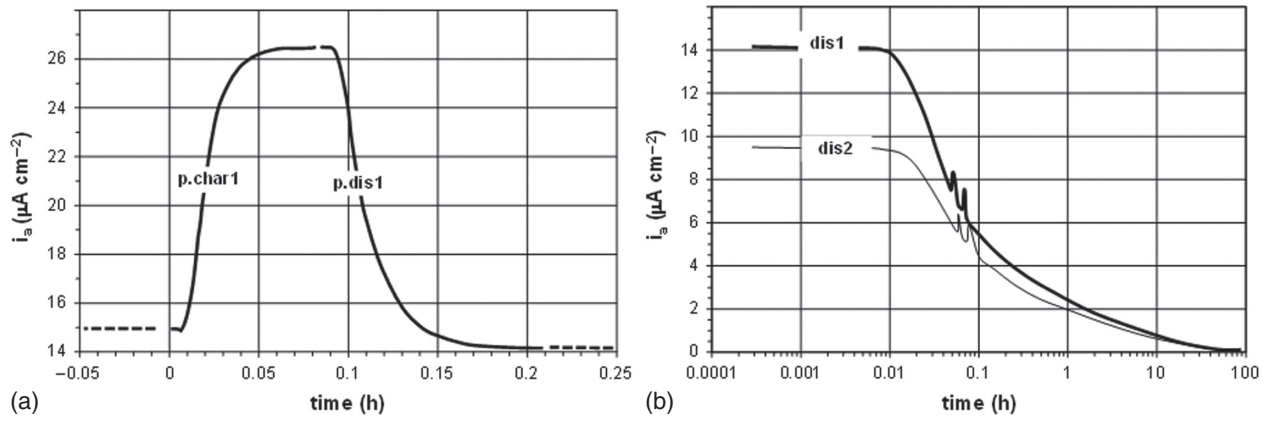

5 Diagram of anodic current density versus time for specimen A3 (X65 annealed, thickness = 1·03 mm) after 100 h of cathodic polarisation: *a* with variation in cathodic current (p.char1: first partial charge, $\Delta i_c = -0{\cdot}5 \rightarrow -1$ mA cm^{-2}; p.dis.1: first partial discharge, $\Delta i_c = -1 \rightarrow -0{\cdot}5$ mA cm^{-2}) and *b* after zeroing cathodic polarisation (logarithmic scale for time)

of i_{max} can the cathodic compartment be emptied, dried and conditioned with a dry N_2 atmosphere.

Fifth, the hydrogen permeation test can be repeated following the same procedure as described in points 2, 3 and 4 and in the related Figs. 4 and 5, which also show the char2 and dis2 phases. In particular, p.char2 and p.dis2, not shown here, have altogether similar, and often perfectly identical, trends to those of p.char1 and p.dis1.[23]

Evaluation of diffusion coefficients

Figure 6 shows an example of the analysis of experimental data relating to the specimen A3 at different experimental steps (different symbols) and the possible interpolations with theoretical curves for different values of D (continuous lines). The following points can be made with regard to Fig. 6, which relates to the specimen A3, but is qualitatively representative of all samples and specimens analysed.

First, the experimental curves p.char1 (▲) and p.dis1 (△) can be superposed almost perfectly, and the theoretical curve interpolates the experimental data very well throughout the relative flux field, yielding a value of $D = D_L = 4{\cdot}5 \times 10^{-9}$ m^2 s^{-1} that can be attributed to the migration of hydrogen in the crystal lattice of the real material.

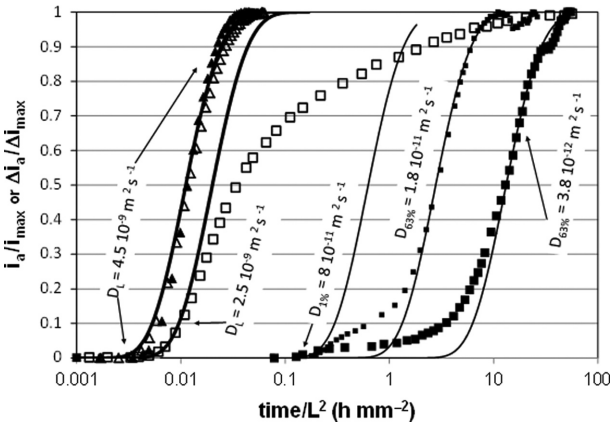

6 Experimental curves i_a/i_{max} and $\Delta i_a/\Delta i_{max}$ versus time/L^2 for A3 (X65 annealed, thickness = 1·03 mm) in different phases of H permeation test and related theoretical curves for different values of *D* that interpolate experimental data (according to various techniques) [■, char1; ■, char2; □, dis1 ($1-i_a/i_{max}$ for relative flux, *see* Fig. 3*b*); ▲, p.char1; △, p.dis1]

Second, the experimental curve dis1 (□) can be interpolated from the theoretical curve only for relative flux values slightly $>0{\cdot}1$ ($\sim$90% of the actual i_{max}) and for $D_L = 2{\cdot}5 \times 10^{-9}$ m^2 s^{-1}, a value similar to that estimated from p.char1 and p.dis1. For relative flux values $>0{\cdot}2$, the experimental flux curve deviates from the theoretical curve owing to the release of hydrogen from the reversible traps with a slower kinetics.

Third, the experimental curves char1 and 2 (■ and ■) describe diffusion processes that are considerably slower than those described above and give rise to a range of values of D, calculated at 1 and 63% of i_a/i_{max}, which differ by more than one order of magnitude.[22,23] The experimental curve obtained in the char1 phase is significantly slowed by the presence of both reversible and irreversible traps, where interactions with hydrogen stabilise over very long times; the curve in the char2 phase is slowed only by the presence of T_{rev} (the T_{irr} were saturated in the char1 phase), so the diffusion process is faster.

Comparison between the various D values considered is problematic, since only those obtained in the dis1 or p.char1 and p.dis1 phases have similar values and meanings. In particular, the D values obtained in char1 and char2, called apparent D or effective D (in particular, $D_{63\%}$), could provide misleading information. In fact, they differ by as much as three orders of magnitude from D_L, which is the most significant value in stationary conditions and is more representative of hydrogen embrittlement under field conditions. The diffusion coefficient D_L is the coefficient with respect to the traps T_L previously identified, i.e. interstitial sites plus the reversible traps with higher capture/release rates. Fallahmohammadi *et al.*[23] show experimental results, along with theoretical curves according to Fick's law, for X65 and F22 steels with three different heat treatment conditions, obtained according to different methods. The diffusion coefficient D_L, obtained in these latter tests, allows us to make the following observations for both steels:

(i) the experimental results, for the three heat treatments, are distributed over three orders of magnitude with respect to the time scale (from values of 0·001 to 1 h mm^{-2})

Table 3 Diffusion coefficient D_L ($m^2\ s^{-1}$) for X65 steel and ratio $D_{L,max}/D_{L,min}$, (3rd line) which can be considered an indicator of data dispersion

Annealing	Quenching and tempering	Water quenching
$(1{\cdot}2–3{\cdot}3)\times10^{-9}$	$(3{\cdot}5–6{\cdot}3)\times10^{-10}$	$(1{\cdot}1–1{\cdot}8)\times10^{-10}$
2·8	1·8	1·6

Table 4 Diffusion coefficient D_L ($m^2\ s^{-1}$) for F22 steel

Annealing	Quenching and tempering	Water quenching
$(1{\cdot}4–1{\cdot}7)\times10^{-9}$	$(6{\cdot}2–6{\cdot}6)\times10^{-10}$	$(1{\cdot}6–2{\cdot}4)\times10^{-10}$

Table 5 Diffusion coefficient D_L ($m^2\ s^{-1}$) for X65 steel (quenched and tempered) as function of plastic strain

0% deformation	6% deformation	22–43% deformation
$(5–6)\times10^{-10}$	$1{\cdot}6\times10^{-10}$	$(5{\cdot}6–6)\times10^{-11}$

(ii) each heat treatment condition is clearly distinguished from the others without any overlap, suggesting that measurement reproducibility is relatively good, that a steady state for diffusion processes is maintained during the measurement and hence that the D_L coefficients obtained from these measurements can be deemed reliable and representative of the diffusion processes; this distinction among different heat treatments was not possible using the apparent or effective diffusion coefficients proposed in ISO 17081

(iii) the theoretical curves interpolate the experimental data very well throughout the relative flux range in the p.char/dis phases, so the D_L values thus obtained are not a function of time during the measurement; the sequence of values predictable for these different metallurgical structures ever richer in 'lattice defects' or traps of a certain type are reported in Tables 3 and 4.

For the deformed X65 sample, using the same procedures, similar results are obtained as the degree of deformation increases (*see* Table 5).[24]

Conclusions

The transport of hydrogen in carbon or low alloy steels can be described by a complex model that takes into account diffusion laws (Fick's) and the phenomena of hydrogen capture and release by different traps. These traps react with permeating hydrogen atoms and are characterised by different reaction kinetics and equilibrium relationships.

The experimental methods and the procedures for determining the hydrogen diffusion coefficient in metals, in particular the Devanathan–Stachurski electrochemical method, must be applied appropriately to measure diffusion coefficients under equilibrium conditions of the traps that better simulate long term charging processes.

For this reason, the partial charge/discharge method proposed by Zakroczymski is the most promising, and in the present work, it was applied to two steels (API 5L X65 and ASTM A182 F22) with different heat treatment conditions and degree of plastic deformation. Within the limits of the 'material–environment' combinations selected for this investigation, we have obtained highly reproducible values of the diffusion coefficient D_L related to the interstitial sites plus the reversible traps with higher capture/release rates, according to the proposed model. In particular, its values decrease:

1. in the order of annealed ($10^{-9}\ m^2\ s^{-1}$), quenched and tempered ($5\times10^{-10}\ m^2\ s^{-1}$) and water quenched ($10^{-10}\ m^2\ s^{-1}$) samples
2. for quenched and tempered X65 steel, as plastic deformation increases (5×10^{-10} to $5\times10^{-11}\ m^2\ s^{-1}$).

References

1. R. A. Oriani, J. P. Hirth and M. Smialowski: 'Hydrogen degradation of ferrous alloys'; 1985, Park Ridge, NJ, Noyes Publications.
2. M. A. V. Devanathan and Z. Stachurski: 'The adsorption and diffusion of electrolytic hydrogen in palladium', *Proc. R. Soc. A*, 1962, **270A**, 90–102.
3. A. Turnbull, M. Saenz De Santa Maria and N. D. Thomas: 'The effect of H_2S concentration and pH on hydrogen permeation in AISI 410 stainless steel in 5% NaCl', *Corros. Sci.*, 1989, **29**, 89–104.
4. Y. F. Cheng: 'Analysis of electrochemical hydrogen permeation through X-65 pipeline steel and its implications on pipeline stress corrosion cracking', *Int. J. Hydrogen Energy*, 2007, **32**, 1269–1276.
5. 'Method of measurement of hydrogen permeation and determination of hydrogen uptake and transport in metals by an electrochemical technique', ISO 17081. 1st edition; 2004, Geneva, Switzerland, ISO.
6. A. McNabb and P. K. Foster: 'A new analysis of the diffusion of hydrogen in iron', *J. Trans. Metall. Soc. AIME*, 1963, **227**, 618–627.
7. R. A. Oriani: 'The diffusion and trapping of hydrogen in steel', *Acta Metall.*, 1970, **18**, 147–157.
8. M. Iino: 'A more generalized analysis of hydrogen trapping', *Acta Metall.*, 1982, **30**, 367–375.
9. M. Iino: 'Analysis of irreversible hydrogen trapping', *Acta Metall.*, 1982, **30**, 377–383.
10. L. Péter, B. Almási, B. Verő and H. Schneider: 'Theoretical analysis of entrapment kinetics in hydrogen permeation experiments', *Mater. Sci. Eng. A*, 2003, **A339**, 245–254.
11. J. B. Leblond and D. Dubois: 'Overview no. 29. A general mathematical description of hydrogen diffusion in steels. I: derivation of diffusion equations from Boltzmann-type transport equations', *Acta Metall.*, 1983, **31**, 1459–1469.
12. J. B. Leblond and D. Dubois: 'Overview no. 29. A general mathematical description of hydrogen diffusion in steels. II: numerical study of permeation and determination of trapping parameters', *Acta Metall.*, 1983, **31**, 1471–1478.
13. A. J. Kumnick and H. H. Johnson: 'Deep trapping states for hydrogen in deformed iron', *Acta Metall.*, 1980, **28**, 33–39.
14. A. H. M. Krom and A. D. Bakker: 'Hydrogen trapping models in steel', *Metall. Mater. Trans. B*, 2000, **31B**, 1475–1482.
15. A. Turnbull, M. W. Carroll and D. H. Ferriss: 'Analysis of hydrogen diffusion and trapping in a 13% chromium martensitic stainless steel', *Acta Metall.*, 1989, **37**, 2039–2046.
16. T. Zakroczymski: 'Adaptation of the electrochemical permeation technique for study entry, transport and trapping of hydrogen in metals', *Electrochim. Acta*, 2006, **51**, 2261–2266.
17. T. Zakroczymski: 'Electrochemical determination of hydrogen in metals', *J. Electroanal. Chem.*, 1999, **475**, 82–88.
18. P. Fassina, F. Bolzoni, G. Fumagalli, L. Lazzari, L. Vergani and A. Sciuccati: 'Influence of hydrogen and low temperature on mechanical behaviour of two pipeline steels', *Eng. Fract. Mech.*, 2012, **81**, 43–55.
19. P. Fassina, L. Lazzari, F. Brunella, G. Re, L. Vergani and A. Sciuccati: 'Effect of hydrogen and low temperature on fatigue crack growth of pipeline steels', *Eng. Fract. Mech.*, 2013, **103**, 10–25.
20. L. Vergani, A. Sciuccati, G. Re and F. Bolzoni: 'Effect of hydrogen environment on fatigue behaviour of high toughness steels', in 'Fatigue crack growth: mechanisms, behavior and analysis', (eds.

P. Tang and J. L. Zhang), 47–95; 2012, Haupage, NY, NOVA Publishers.
21. E. Fallahmohammadi, F. Bolzoni and L. Lazzari: 'Measurement of lattice and apparent diffusion coefficient of hydrogen in X65 and F22 pipeline steels', *Int. J. Hydrogen Energy*, 2013, **38**, 2531–2543.
22. E. Fallahmohammadi, F. Bolzoni, G. Fumagalli, G. Re and L. Lazzari: 'Diffusione e intrappolamento dell'idrogeno in acciai per condotte (Diffusion and trapping of hydrogen in pipeline steels)', *La Metall. Ital.*, 2013, **105**, (10), 3–13.
23. E. Fallahmohammadi, F. Bolzoni, G. Fumagalli, G. Re, G. Benassi and L. Lazzari: 'Hydrogen diffusion into three metallurgical microstructures of a C–Mn X65 and low alloy F22 sour service steel pipelines', *Int. J. Hydrogen Energy*, 2014, **39**, 13300–13313.
24. E. Fallahmohammadi, F. Bolzoni, M. Ormellese, G. Re, G. Fumagalli, R. G. Ballinger, L. Lazzari, Proc. Conf. Corrosion 2014, San Antonio, TX, USA; March 2014, National Association of Corrosion Engineers. Paper 4390.
25. 'Specification for line pipe', API Specification 5L; 2004, Washington, DC, USA, American Petroleum Institute.
26. 'Specification for forged or rolled alloy-steel, pipe flanges, forged fittings and valves and parts for high-temperature service', A-182; 2004, West Conshohocken, PA, USA, ASTM International.
27. E. Fallahmohammadi: 'Diffusion and trapping of hydrogen in pipeline steels', PhD thesis in Materials Engineering, Politecnico di Milano, Milan, Italy; 2014.
28. M. A. V. Devanathan and Z. Stachurski: 'The mechanism of hydrogen evolution on iron in acid solutions by determination of permeation rates', *J. Electrochem. Soc.*, 1964, **111**, (5), 619–623.
29. P. Manolatos, M. Jerme and J. Galland: 'Necessity of a palladium coating to ensure hydrogen oxidation during electrochemical permeation measurements on iron', *Electrochim. Acta*, 1995, **40**, 867–887.
30. L. Nanis and T. K. G. Namboodhiri: 'Mathematics of the electrochemical extraction of hydrogen from iron', *J. Electrochem. Soc.*, 1972, **119**, 691–694.
31. S. Serna, H. Martinez, S. Y. Lopez, J. G. Gonzalez-Rodriguez and J. L. Albarran: 'Electrochemical technique applied to evaluate the hydrogen permeability in microalloyed steels', *Int. J. Hydrogen Energy*, 2005, **30**, 1333–1338.
32. M. F. Stevens and I. M. Bernstein: 'Microstructural trapping effects on hydrogen induced cracking of a microalloyed steels', *Metall. Trans. A*, 1989, **20A**, 909–919.
33. G. M. Pressouyre and I. M. Bernstein: 'Quantitative analysis of hydrogen trapping', *Metall. Trans. A*, 1978, **9A**, 1571–1580.
34. J. Lamb, V. Arjunan, V. Deodeshmukh, D. Chandra, J. Daemen and R. B. Rebak: 'Hydrogen diffusion and trapping effects in low and medium carbon steels for subsurface reinforcement in the proposed Yucca mountain repository', *Metall. Mater. Trans. A*, 2007, **38A**, 348–355.